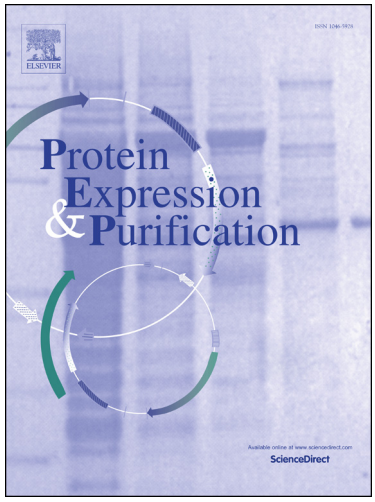

Biophysical characterization of the outer membrane polysaccharide export protein and the polysaccharide co-polymerase protein from *Xanthomonas campestris*

M.I. Bianco, M. Jacobs, S.R. Salinas, A.G. Salvay, M.V. Ielmini, L. Ielpi

PII: S1046-5928(14)00137-5
DOI: http://dx.doi.org/10.1016/j.pep.2014.06.002
Reference: YPREP 4521

To appear in: *Protein Expression and Purification*

Received Date: 25 February 2014
Revised Date: 26 May 2014

Please cite this article as: M.I. Bianco, M. Jacobs, S.R. Salinas, A.G. Salvay, M.V. Ielmini, L. Ielpi, Biophysical characterization of the outer membrane polysaccharide export protein and the polysaccharide co-polymerase protein from *Xanthomonas campestris*, *Protein Expression and Purification* (2014), doi: http://dx.doi.org/10.1016/j.pep.2014.06.002

Biophysical characterization of the outer membrane polysaccharide export protein and the polysaccharide co-polymerase protein from *Xanthomonas campestris*

M.I. Bianco[a,1,§], M. Jacobs[a,§], S.R. Salinas[a,2], A.G. Salvay[b,c], M.V. Ielmini[a,3], and L. Ielpi[a,*]

Authors´ affiliations: [a]Laboratory of Bacterial Genetics, Fundación Instituto Leloir, IIBBA-CONICET (C1405BWE) Ciudad de Buenos Aires, Argentina. [b]Institute of Physics of Liquids and Biological Systems, Universidad Nacional de La Plata, La Plata (B1900BTE) Buenos Aires, Argentina, [c]Department of Science and Technology, Universidad Nacional de Quilmes, Bernal (B1876BXD) Buenos Aires, Argentina.

*Correspondence to: Luis Ielpi, Fundación Instituto Leloir. Av. Patricias Argentinas 435 (C1405BWE) Buenos Aires, Argentina. Phone: (+5411) 5238-7500. Fax: (+5411) 5238-7501.E-mail: Lielpi@leloir.org.ar

§ Both authors contributed equally to this work

Present address:

[1] M.I. Bianco, Instituto de Ciencia y Tecnología Dr. César Milstein, Fundación Pablo Cassará, CONICET, Saladillo 2468 (C1440FFX) Buenos Aires, Argentina.

[2] S.R. Salinas, Laboratorio de Estructura y estabilidad de proteínas en membranas lipídicas, Centro de Investigaciones en Química Biológica de Córdoba, Universidad Nacional de Córdoba. Ciudad Universitaria (5000) Córdoba, Argentina.

[3] M.V. Ielmini, Alberta Ingenuity Centre for Carbohydrate Sciences, Department of Biological Sciences, University of Alberta, Edmonton, AB, T6G 2E9, Canada.

Abbreviations: Xc, *Xanthomonas campestris*; OPX, outer membrane polysaccharide export; PCP, polysaccharide co-polymerase; TMS, transmembrane segment; SEC, size-exclusion chromatography; SLS, static light scattering; AUC, analytical ultracentrifugation; SV, sedimentation velocity; DDM, n-dodecyl β-d- maltopyranoside; DSP, dithiobis(succinimidyl propionate); DTT, dithiothreitol; PMSF, phenylmethylsulfonyl fluoride; CD, circular dichroism; MALDI-TOF MS, Matrix-Assisted Laser Desorption/Ionization Time-Of-Flight Mass Spectrometry

ABSTRACT

This study investigated the structural and biophysical characteristics of GumB and GumC, two *Xanthomonas campestris* membrane proteins that are involved in xanthan biosynthesis. Xanthan is an exopolysaccharide that is thought to be a virulence factor that contributes to bacterial in planta growth. It also is one of the most important industrial biopolymers. The first steps of xanthan biosynthesis are well understood, but the polymerization and export mechanisms remain unclear. For this reason, the key proteins must be characterized to better understand these processes. Here we characterized, by biochemical and biophysical techniques, GumB, the outer membrane polysaccharide export protein, and GumC, the polysaccharide co-polymerase protein of the xanthan biosynthesis system. Our results suggested that recombinant GumB is a tetrameric protein in solution. On the other hand, we observed that both native and recombinant GumC present oligomeric conformation consistent with dimers and higher-order oligomers. The transmembrane segments of GumC are required for GumC expression and/or stability. These initial results provide a starting point for additional studies that will clarify the roles of GumB and GumC in the xanthan polymerization and export processes and further elucidate their functions and mechanisms of action.

Keywords: membrane proteins; xanthan; *Xanthomonas campestris*; exopolysaccharide

Highlights

- We report the biochemical and biophysical characterization of the membrane proteins GumB and GumC of *Xanthomonas campestris*.
- The recombinant GumB shows to be a tetrameric protein.
- Native and recombinant GumC showed oligomeric conformation.
- Transmembrane segments of GumC are required for its expression and/or stability and oligomerization.

INTRODUCTION

The first steps of bacterial polysaccharide biosynthesis are well understood, but the mechanisms involved in polymerization and export through the cell membrane remain unclear. However, it is well known that membrane proteins are involved in these processes [1]. Xanthan is an exopolysaccharide of high molecular weight produced by *Xanthomonas* spp that is thought to be a virulence factor that contributes to bacterial in planta growth and that plays a role in biofilm formation [2-4]. Moreover, xanthan is one of the most important biopolymers in various industries because of its unique rheological properties [5,6]. Xanthan is synthesized through a Wzy-dependent pathway [7,8] and requires 12 proteins encoded by the gum operon [9,10]. Proteins implicated in repeat unit synthesis (GumDFGHIKLM) have been identified based on experimental data [11-15] while GumE, GumB, and GumC are proposed to be involved in xanthan polymerization and export, and GumJ has been postulated to be the flipase in this system [9,16,17]. Permeabilized *Xanthomonas campestris* (Xc) cells synthesize the repeat units but do not produce xanthan when *gumB* or *gumC* are inactivated [14]. In addition, *gumB* and *gumC* mutants uncouple synthesis of the lipid-linked repeat unit from the polymerization process, and co-overexpression of both proteins results in longer xanthan chains and a more viscous exopolysaccharide. These data suggest that GumB and GumC are needed for xanthan polymerization and export and that they may interact [16]. However, their mechanisms of action remain unknown.

GumB is a lipoprotein that is classified as an outer membrane polysaccharide export (OPX) protein [1]. There is currently structural information about only two OPX proteins, GfcC from *Escherichia coli* [18] and Wza from *E. coli* K30 [19], which are involved in the export of group 1 and group 4 capsular polysaccharides, respectively. GumB contains the polysaccharide polyexport sequence (PES) motif (Pfam 02563) that is characteristic of the OPX proteins [1]. GumB aligns with the residues 67 to 253 of Wza (E value: 2e-13 and

identity: 29%), but transmembrane segments could not be found in GumB by *in silico* prediction. However, GumB locates in membrane fractions in subcellular location experiments as we described in a previous work [16]. GumC is an inner membrane protein belonging to the polysaccharide co-polymerase (PCP) protein family that is classified as being within the PCP2a sub-family [1]. Despite their low sequence homology, PCP proteins are distinguished by their common topology, which consists of a large periplasmic domain that is flanked by two transmembrane segments (TMSs) [1]. The PCP2a proteins have an additional C-terminal cytoplasmic domain with tyrosine autokinase activity [1,20]. GumC topology has been confirmed experimentally to comprise a periplasmic region flanked by two TMSs; however, there is no C-terminal cytoplasmic kinase domain [16], and no obvious kinase partner has been identified on the *Xanthomonas* chromosome [1].

To understand how xanthan polymerization and export occurs, the proteins that are involved in these processes must be characterized. In a previous work, we described the purification and crystallization of a soluble form of GumB. The crystals diffracted at 2.54 Å and we observed that in the crystal GumB is a tetramer [21]. The aim of this study was to further characterize the structure and organization of GumB and to obtain the first insight in the characterization of GumC. We conducted biochemical and biophysical studies, and here we present the first structural insights into these two membrane proteins.

MATERIALS AND METHODS

Materials and general procedures

Proteins were separated by sodium dodecyl sulphate-polyacrylamide gel electrophoresis (SDS-PAGE). Purified proteins, whole bacteria, or membrane preparations were solubilized with 2x denaturing buffer (10 M urea, 2% SDS, and 100 mM Tris-HCl, pH 8.2) and analyzed by SDS-PAGE using 10% gels (unless otherwise indicated) followed either by Coomassie

Blue staining or by transfer to polyvinyl difluoride (PVDF) membranes for immunoblot analysis. Immunoblot analysis was performed using polyclonal mouse anti-GumB or polyclonal rabbit anti-GumC generated in our laboratory [16] as the primary antibodies. Goat anti-mouse or goat anti-rabbit IgG peroxidase-conjugated antibodies (Sigma-Aldrich, Buenos Aires, Argentina) were used as secondary antibodies. Immunoblots were developed with ECLPlus chemoluminescent substrate according to the manufacturer's recommendations (GEHealthcare, Buenos Aires, Argentina). Protein concentration was determined by absorbance at 280 nm using a NanoDrop 2000 Spectrophotometer (Thermo Scientific, Rockford, IL, USA). The subcellular localization of proteins was analyzed by differential centrifugation [11]; each subcellular fraction was subjected to SDS-PAGE and analyzed by either Coomassie Blue staining or immunoblot.

Bacterial strains, media, and plasmids

E. coli DH5α was used for DNA cloning and for overexpressing GumB-His as described previously [21], whereas GumC-His was cloned into *E. coli* DH5α and overexpressed in *E. coli* BL21(DE3). The Xc strains were used for complementation assays and for in vivo cross-linking assays. The wild type and mutant Xc strains used in this study are listed in Table I. The inactivation of the *gumC* gene was obtained in a phosphomano- phosphoglucomutase deficient strain (Xc3188) because its inactivation in the wild-type strain XcFC2 appeared to be lethal [14].

E. coli cells were grown in Luria Bertani (LB) or Terrific Broth (TB) media [22] at 37°C with shaking at 200 rpm. Xc cells were grown in Yeast extract-Malt extract (YM) medium [23] at 28°C with shaking at 200 rpm. Antibiotics were used at the following concentrations when needed: for *E. coli*, 30 μg/mL kanamycin and 100 μg/mL ampicillin; for Xc, 50 μg/mL kanamycin, 30 μg/mL gentamicin, and 5 ug/mL tetracycline. When necessary, isopropyl-β-D-

1-tiogalactopiranósido (IPTG) (Gold Biotechnology, St. Louis, MO, USA) or L-arabinose (Calbiochem, Buenos Aires, Argentina) was added at the indicated concentrations to cultures to induce protein overexpression.

The plasmids used in this study are listed in Table I. In this work we use the corrected sequence for *gumB* (GeneBank AF427012) and for gumC (AF427011) [16]. The pQE30-GBHis was obtained as described by Patel et al. [24], while pET-GCHis was derived from pET28a(+) (Promega) and engineered to encode the C-terminal His_6-tagged GumC fusion protein. The *gumC* gene was amplified from the Xc genomic DNA region that had been cloned into plasmid pBBR5-BC. We used primers FGC28.HisCt and RGC28.HisCt for *gumC* (Table II). The amplified gumC PCR product was digested with NcoI/XhoI and cloned into the corresponding sites of the expression vector. The pBBad-B, pBBad-C, and pBBad-CHis plasmids were generated to express these proteins in Xc cells. The pBBad-B and pBBad-C plasmids were obtained as described by Galván et al. [16]. To generate pBBad-CHis, the gumC gene was amplified from the Xc genomic DNA region that was cloned into plasmid pBBR5-BC using primers FGC28.HisCt and RGC22HisCt (Table II). This added a hexahistidine-tag to the C-terminal end of the protein. PCR product was digested with *NcoI* and *HindIII* and ligated into the corresponding sites of pBBad22K.

The construct sequences were confirmed by DNA sequencing (DNA sequencing service, Fundación Instituto Leloir).

Purification of the recombinant GumB-His and GumC-His fusion proteins

The expression conditions for GumB and GumC were determined by experimenting with conditions to determine the temperature, growth time, induction concentrations, plasmids, and expression strains that would result in protein expression.

The recombinant GumB-His fusion protein was overexpressed in *E. coli* DH5α (pRep4) and purified as described by Jacobs et al. [21] GumC-His and was overexpressed in *E. coli* BL21(DE3)/pETGumC-His and subjected to a two-step chromatographic purification protocol. GumC-His overexpression was performed by inoculating 20 ml of starter culture (grown for 4 h at 37ºC) into a liter of TB medium followed by culture to late-log phase (OD_{600} 0.5). At this point, the culture was transferred to 20°C for 30 min, and protein expression was induced by adding 0.5 mM IPTG and culturing for an additional 18–20 h. Cells were harvested and washed twice with 50 mM Tris-HCl 10 mM $MgCl_2$, pH 8.0. Cells expressing GumC-His were suspended in 20 ml of suspension buffer [Tris-HCl 50 mM, pH8.0, 0.5 M NaCl, 10% (v/v) glycerol, 1 mM phenylmethylsulfonyl fluoride (PMSF, Sigma)] per liter of culture and disrupted by three passages through a French pressure cell at 110 MPa at 4ºC. Unbroken cells, cellular debris, and inclusion bodies were removed by differential centrifugation. Membrane fractions were separated by ultracentrifugation for 2 h at 100,000 × g at 4ºC and stored at -20°C until use. Membranes were thawed, suspended in lysis buffer [50 mM Tris-HCl, pH 8.0, 0.5 M NaCl, 10% (v/v) glycerol, 8.5 mM n-dodecyl β-D-maltopyranoside (DDM; Anatrace), and 1 mM PMSF], incubated with gentle agitation at 4ºC for 2 h, and centrifuged for 2 h at 100,000 x g at 4ºC.

The solubilized membrane extract containing GumC-His was applied to a nickel HiTrap Chelatin HP (GE-Healthcare) column pre-equilibrated with buffer A [20 mM TrisHCl, pH8.0; 0.85 mM DDM; 0.5 M NaCl; 10% (v/v) glycerol; 10 mM imidazole]. Bound proteins were eluted with a gradient of 10–350 mM imidazole in buffer A. Fractions with >25% GumC-His protein were pooled and applied to a Superdex 200 prep grade size-exclusion chromatography column (GE Healthcare) pre-equilibrated with buffer B [20 mM Tris-HCl, pH 8.0, 0.85 mM DDM, 0.5 M NaCl, 15% (v/v) glycerol]. A Jasco FPLC system connected to a UV-1575 Intelligent UV–Vis detector was used for the nickel chelating and SEC columns. Elution of

proteins was analyzed by Coomassie blue staining of SDS-PAGE gels and by immunoblotting. GumC-His was concentrated using 100,000 MWCO regenerated cellulose centrifugal filters (Amicon Ultra, Millipore, Billerica, MA, USA).

Size exclusion chromatography coupled to static light-scattering (SEC-SLS)

Protein samples were loaded onto a Superdex 200 (GE-Healthcare) column connected to a Precision Detectors PD2010 light-scattering instrument that was connected in tandem to a LKB 2248 high-performance liquid chromatography and to a Waters 486 UV-detector.

GumB-His was applied to a column that was equilibrated with 50 mM Tris-HCl (pH 8.0), 150 mM NaCl, and 0.17 mM DDM, while GumC-His was applied to a column equilibrated with buffer B. The absorbance at 280 nm, the 90° light scattering, and the refractive index signals of the eluting material were recorded and analyzed with the Discovery32 software that was supplied by Precision Detectors. Background subtraction was performed using data from protein-free buffer. The molecular mass of the proteins was calculated by the three detectors method [25] using BSA (30 μM) as a standard. We analyzed samples of GumB-His (40, 200, and 400 μM) and GumC-His (18, 90, and 180 μM). Both proteins were studied in buffers that had different ionic strengths. Prism 5 (GraphPad, San Diego, CA) was used for plotting and curve fitting data from the SEC-SLS experiments.

Chemical cross-linking

The purified GumB-His and GumC-His proteins were exchanged by ultrafiltration (10,000 and 100,000 MWCO Amicon Ultra Millipore, Billarica, MA, USA, respectively) into 20 mM sodium phosphate buffer (PBS), pH 8.0, containing 150 mM NaCl and 0.17 mM DDM for GumB-His, and 500 mM NaCl, 15% glycerol, and 0.85 mM DDM for GumC-His. Both proteins were analyzed at concentrations of 1, 5, and 10 μM. Dithiobis(succinimidyl)

propionate (DSP; Pierce, Thermo Scientific, Rockford, IL, USA) was used as cross-linking agent. Different reaction times, reaction temperatures, and cross-linker concentrations were assayed to optimize the reaction conditions for each protein. To study protein stability as a function of temperature, cross-linking experiments were carried out in a temperature range of 5 to 70°C at intervals of 5°C. Samples were equilibrated for 10 min at each temperature before adding 0.2 mM DSP. Reactions were evaluated by Coomassie Blue staining of SDS-PAGE gels. For *in vivo* chemical cross-linking, intact Xc cells were grown in YM to OD_{600} 0.7, washed with PBS (pH 7.2), and concentrated 5-fold in PBS. The cross-linking was carried out with 0.5 mM DSP for 30 min on ice [26,27]. Cells were harvested and suspended in 2x denaturing buffer. Samples were analyzed by immunoblotting. *In vitro* and *in vivo* cross-linking reactions were stopped by the addition of 50 mM Tris-HCl, pH 7.5. To control for specific DSP-dependent cross-linking, we reversed the cross-linking by adding 50 mM dithiothreitol (DTT; Sigma-Aldrich). The use of reducing agents to revert the cross-linking was possible because GumC do not contain cysteine residue and, although the cysteine residue (lipidation signal) is still present in GumB-His, it is not involved in any DTT-sensitive effects seen during cross-linking. As control, we carried out SDS-PAGE experiments under reducing and non-reducing conditions and the pattern obtained in both cases were similar, suggesting that oligomers formation in presence of DSP is specific for this cross-linker agent.

Analytical ultracentrifugation (AUC) sedimentation velocity (SV)

The AUC SV experiments were performed using solutions of 400 µM GumB-His in 50 mM Tris-HCl (pH 8.0), 150 mM NaCl, and 0.17 mM DDM (1 CMC) or 185 µM GumC-His in 20 mM Tris-HCl (pH 8.0), 500 mM NaCl, 15% glycerol, and 0.85 mM DDM (5 CMC). All experiments were performed on an analytical ultracentrifuge XLI (Beckman Coulter, Palo Alto, CA, USA) using an Anti-60 rotor with a rotor speed of 42,000 rpm at 20°C, typically

overnight. We used double-sector cells of optical path length 3- and 1.5-mm equipped with sapphire windows. The acquisition software Proteomelab XLI V6.0 was used, and acquisitions were performed using absorbance at 280 and interference optics. The analyses of AUC SV data were performed using SEDFIT software (version 13c from P. Schuck; http://www.analyticalultracentrifugation.com).

The density (ρ°) and viscosity (η°) of the buffer, which are required for AUC SV analysis, were calculated with SEDNTERP software from John Philo (http://www.jphilo.mailway.com/). The partial specific volume ($\bar{v}$) of peptides was calculated from the amino acid sequences using SEDNTERP. Analyses of AUC SV experiments were performed using the continuous distribution *c(s)* model analysis of SEDFIT.

According to the theoretical formalism of AUC SV [28], for each species that sediments in solution, the sedimentation coefficient *(s)* and the diffusion coefficient (*D*) are related by the Stokes-Einstein and Svedberg equations to the molecular mass (*M*) and the hydrodynamics radius (R_H): $R_H=RT/(N_A 6\pi\eta^\circ D)$and $M=RTs/[D(1-\rho^\circ \bar{v})]$, where R is the gas constant, T the absolute temperature, N_A Avogadro's number. *s* and *D* can be corrected for the solvent conditions to $s_0^{20,w}$ and $D_0^{20,w}$, i.e. to water at 20°C. The frictional ratio f/f_{min} is the ratio of the hydrodynamic radius to the radius of the anhydrous volume: $R_H=(f/f_{min})R_{min}$. The former describes the size (dimension) of the molecule in solution, and the latter depends on the cubic root of the molar mass. The frictional ratio f/f_{min} depends on the hydration, surface roughness, shape, and flexibility of the particle. For globular compact macromolecules (which is what is expected for protein-detergent complexes), its value is nearly constant around 1.25. The amount of detergent bound to the membrane proteins was determined by the ratio between the interference signal and the absorbance signal as described previously [28].The SV profiles, which were acquired with absorbance and interference optics, were analyzed by the *c(s)*

analysis using the SEDFIT program. For GumB-His and GumC-His, the Lamm equation was simulated for 200 particles in the ranges (0 S, 25 S) and (0 S, 14 S), respectively, with a partial specific volume of 0.74 ml g^{-1} for GumB-His and an estimated value of 0.78 ml g^{-1} for the complex of GumC-His with bound DDM.

Circular dichroism (CD) spectroscopy

CD studies were performed using a Jasco J-810 spectro-polarimeter equipped with a Peltier temperature control system. Far-UV CD spectra were collected on a 0.1-cm path length quartz cuvette (Hellma) at 5 and 20°C, with a scan speed of 100 nm/min, a response time of 2 seconds, and a bandwidth of 2 nm, in a range of 200 to 260 nm, using a protein concentration of 10 µM for GumB-His and 5 µM for GumC-His. All spectra represent an average of at least five scans.

Protein thermal denaturation was measured in the far-UV CD spectrum. For thermal scans, the protein samples were heated from 5 to 95°C and subsequently cooled to 5°C with a heating/cooling rate of 2°C/min as controlled by a Peltier temperature control system. Far-UV CD measurements were recorded every 1°C, and the dichroic activity was monitored every 1°C with 2 seconds average time. The melting points were determined by calculating the first derivative of the experimental curve. GumB-His thermal denaturation was analyzed by fitting it to a two-state model according to Santoro and Bolen [29].

We analyzed the GumB-His and GumC-His proteins using far-UV CD spectroscopy in the presence of 0.01, 0.001, and 0.0001% xanthan. Each recombinant protein was incubated with xanthan for different times (range: 10 min to 24 h). Protein thermal denaturation was also studied in the presence of 0.01% xanthan as described above.

All spectra were corrected for solvent contribution. Background subtraction was performed using protein-free buffer or protein-free buffer plus xanthan for CD spectra measurements and for thermal denaturation experiments. CD values were converted to mean residue ellipticity (MRE) in units of degree.cm^2.dmol^{-1} using standard procedures. Prism 5 (GraphPad, San Diego, CA) was used for plotting and curve fitting in the CD experiments.

Limited proteolysis

Purified GumB-His and GumC-His in absence and presence of 0.01% of xanthan were partially digested by trypsin (Sigma). Controlled proteolytic digestion was carried out at 20°C and at a final protein concentration of 40 µM for GumB-His and 18 µM for GumC-His and aliquots were analyzed at different reaction times. Before digestion, GumB-His and GumC-His were incubated for 10 min at 20°C. Proteolysis was carried out using trypsin:GumB-His and trypsin:GumC-His ratios of 1:50 and 1:200 (w/w), respectively. Samples were vortexed briefly and incubated at 20°C in a water bath. Aliquots of proteins were taken at different time points. At each time point, the proteolysis reaction was quenched immediately by adding denaturing buffer with 100 mM PMSF, heating the reaction to 100°C for 10 min, and then storing the samples at -80ºC until analysis. The time courses and the extent of cleavage of the proteolytic digestions were analyzed by SDS- PAGE. Samples were separated by 16% SDS-PAGE for GumB-His and 10% SDS-PAGE gels for GumC-His followed by gel staining with Coomassie Brilliant Blue solution.

Matrix-Assisted Laser Desorption/Ionization Time-Of-Flight Mass Spectrometry (MALDI-TOF MS)

In order to determine the presence of glycosilation in GumC-His, it was analyzed by MALDI TOF MS at the Institut de Biologie Structurale (Mass Spectrometry Platform), Grenoble, France. A sample of 10 mg/ml purified GumC-His was diluted 1:10 in sinapinic acid matrix

(10 mg/ml in acetonitrile/water-0.1% TFA (50:50)) and 2 µl were deposited directly on the target. The sample was analyzed on a MALDI TOF MS (Autoflex, Bruker Daltonics), operated in linear positive mode (LP_QC_03.par).

RESULTS

Expression and purification of the recombinant GumB-His and GumC-His proteins

GumB is initially translated as a precursor in the cytoplasm with an N-terminal signal peptide of 25 amino acids that has a conserved signal peptide. After translocation across the inner membrane, pro-GumB is processed by binding of a lipid moiety to the N-terminus and subsequent removal of the signal peptide, which results in the mature lipidated protein. First we tried to overexpress lipidated GumB. Although it could be overexpressed without lethal effects, its expression in *E. coli* was not detectable by SDS-PAGE. XcFC2/pBBad-B cells showed higher GumB expression, but a very low proportion of it was located in the outer membrane fraction (data not shown). We reported previously that we could overexpress and purify GumB that lacked its signal peptide (GumB-His) and that had a hexahistidine-tag (His_6-tag) at its N-terminal end; this protein was purified using a two-step chromatographic protocol [21]. GumB-His was obtained as a unique protein band (~24 kDa) without degradation products and that yielded 20 mg of protein per liter of culture [Fig. 1(A)].

For GumC, we overexpressed the full-length protein with a His_6-tag at its C-terminal end (GumC-His) and purified it via a two-step protocol that was based on affinity and size exclusion chromatography. SDS-PAGE and immunoblot analyses of GumC-His showed unique ~53-kDa protein band with no degradation products that was > 95% pure [Fig. 1(B) and (C)]. This method had a yield of 2 mg of purified protein per liter of culture. Because we do not dispose of any method to measure GumC activity *in vitro*, we carried out complementation assays. We verified that the amino acid sequence of GumC-His is able to

restore xanthan synthesis in the *gumC* mutant strain (data not shown). This result supports that the amino acid sequence used for the recombinant GumC-His has the functionality if the protein is properly folded in *E. coli.*

Figure 1

Oligomerization state of GumB-His and GumC-His

To investigate the quaternary structure of GumB and GumC, we studied both proteins using *in vitro* and *in vivo* chemical cross-linking, SEC-SLS, and analytical ultracentrifugation AUC SV experiments.

GumB-His and GumC-His were each cross-linked by incubation with 0.2 mM DSP for 1 min on ice. On SDS-PAGE, cross-linked GumB-His migrated at ~50, ~75, and ~100 kDa [Fig.2(A)], while cross-linked GumC-His showed bands between 100 and 150 kDa and at ~225 kDa [Fig. 2(B)]. For both proteins, a fraction of GumB-His and GumC-His migrated as monomers at ~24 kDa and ~53 kDa, respectively. After DTT addition to reverse the cross-linking, both proteins returned to their monomeric states, and in the absence of DSP, both migrated mainly as monomeric proteins [Fig. 2(A) and (B)]. These results suggest that both proteins oligomerize or form protein aggregates *in vitro*. In addition, active XcFC2 cells were treated with DSP, and the resulting oligomeric forms were analyzed by immunoblotting. The oligomeric conformation of GumB could not be determined. We observed high molecular mass complexes or aggregates that did not enter or load onto the gels suggesting that, in its native environment, GumB might form higher molecular mass homo-oligomers or that it might interact with other XcFC2 proteins (data not shown). Immunoblots probed with anti-GumC showed bands migrating between 130 and 170 kDa as well as higher molecular mass oligomers [Fig. 2(C)]. This result suggests that GumC might form homo-oligomers or that it might form complexes with other XcFC2 proteins. To investigate whether the His_6-tag

interferes with the oligomerization of GumC-His, Xc3188C/pXanA cells complemented with pBBad-CHis were subjected to *in vivo* cross-linking with DSP. Results that were similar to those observed in the XcFC2 strain were obtained (data not shown), indicating that the His_6-tag did not interfere with the oligomerization.

The conformational homogeneity of the purified GumB-His and GumC-His proteins were studied by SEC-SLS and their molecular mass were calculated by the three detector method. GumB-His showed an average value of ~100 kDa, which is consistent with the predicted mass of a tetrameric protein [Fig. 2(D)], while GumC-His showed values between ~69 and ~95 kDa, corresponding to~1.3- to ~1.8-fold higher than the molecular mass of the monomer [Fig. 2(E)]. In light of these results, we subjected GumC-His to MALDI-TOF MS analysis to confirm its expected molecular mass. GumC-His showed a molecular mass of 53.758 kDa when the expected molecular mass was 53.792 kDa. Mass measurement accuracy (663 ppm) is within the accepted values (300-1000 ppm). This result showed that GumC-His is not a glycosylated protein [Fig. 2(F) and (G)].

Figure 2

AUC SV experiments were also performed to better characterize the two membrane proteins in solution. The SV profiles of GumB-His and GumC-His were analyzed in terms of particle distribution using *c(s)* analysis [Fig. 3(A) and (B)]. The *c(s)* analysis of GumB-His showed similar distributions of the sedimentation coefficients *(s)* no matter which optics were used [Fig. 3(A)]. GumB-His showed a main contribution at 4.9 S, corresponding to 65% of the signal, and a second contribution at ~7.1 S, corresponding to 12% of the signal. Considered as a whole, the species above the main peak at 4.9 S had a mean sedimentation coefficient of 0.3 S and accounted for 34% of the signal. These larger species were most likely protein aggregates. A minor contribution was detected at ~3 S, which might be due to impurities or to

a limited amount of DDM-solubilizing impurities. The ratio between the interference signal and the absorbance signal allows one to determine the amount of detergent bound to the species [28]. In this case, DDM was not detected bound to GumB-His. According to the Stokes-Einstein and Svedberg equations, if we consider the hypothesis that GumB-His is a tetramer of molecular mass of ~100-kDa (as suggested by our *in vitro* chemical cross-linking and SEC-SLS experiments), we calculated a frictional ratio (*f/fmin*) of 1.4 (corresponding to a slightly anisotropic shape) in order to have a sedimentation coefficient of ~4.9 S. Assuming this f/f_{min} value, and assuming that GumB-His is not a globular protein and that it can have a slightly anisotropic shape, the SV results indicate that the main contribution at 4.9 S in the *c(s)* distribution corresponds to a tetrameric protein of ~100 kDa without any bound DDM. Similar results were observed on diluted samples of GumB-His.

On the other hand, *c(s)* analysis of GumC-His above 1.5 S showed a distribution of contributions that corresponded to different species, with a main contribution at ~2 S, a shoulder at ~3 S, and minor contributions at ~6 S that were associated with larger species [Fig. 3(B)]. The species that sediment at ~2 S and 3 S together comprised at least the 70% of the total signal (~55% and ~15%, respectively), while the remaining 30% corresponded to larger species that were thought to be aggregates. Looking at the full range of the sedimentation coefficients, interference showed a main contribution at 1.2 S ($s^{20,w}$= 2.9 S).

The experimental value for DDM micelles measured in water ($s^{20,w}$ = 2.9 S) [30] is close to that observed for the buffer used to dilute the protein. Absorbance data showed a minor contribution at the same value of s = 1.2 S, which might correspond to a limited number of DDM micelles that solubilized impurities. Using the ratio between the interference signal and the absorbance signal, we determined that the amount of bound detergent was 0.65±0.25 g of DDM per g of GumC-His. Taking into account the molecular mass of GumC-His and the

amount of bound detergent, we determined from the relationships specified by SV theory [28] that the main contribution at ~2 S observed above 1.5 S corresponded to GumC-His monomers and that the shoulder at ~3 S corresponded to dimers. SV experiments performed on diluted samples showed similar results.

Figure 3

Secondary structure analysis and thermal denaturation experiments

The far-UV CD spectrum of GumB-His showed a negative peak at ~210 nm with a less intense shoulder between 213 and 220 nm [Fig. 4(A)], while GumC-His showed a far-UV CD spectrum with minima at ~208 and ~222 nm [Fig. 4(B)]. The secondary structure content could not be estimated for either protein since the spectra showed high dynode voltage between 190 and 200 nm.

The relative stability of the two proteins was assessed by following changes in the far-UV CD spectra with increasing temperature. Thermal denaturation of GumB-His resulted in a curve with a sigmoid shape, indicating cooperative unfolding, and a melting point of 39.9±0.2°C [Fig. 4(C)]. This reflected the stability of GumB-His at the temperatures used for biophysical and structural studies. The far-UV CD melting curve of GumC-His showed a non-cooperative unfolding [Fig. 4(D)]. Both the GumB-His and the GumC-His unfolding processes were irreversible. To investigate why they were irreversible, dynode voltage (turbidity) was recorded while solutions of GumB-His or GumC-His were heated. In both cases we observed a large irreversible heat-induced increase in dynode voltage, which indicates aggregation. In addition, the turbidity changes clearly correlated with protein unfolding as monitored by far-UV CD, confirming that GumB-His and GumC-His aggregate when the temperature is increased. The subsequent reduction in dynode voltage observed upon heating to >35ºC for

GumB-His and to >45ºC for GumC-His reflects precipitation of the heat-unfolded proteins [Fig. 4(C) and (D)].

We also analyzed the thermal stability of both proteins using cross-linking with DSP. As the temperature increased, GumB-His aggregated leading to high molecular mass complexes that did not enter the SDS-PAGE gels [Fig. 4(E)]. This indicates that the protein aggregates quickly after it unfolds. A white precipitate was observed after GumB-His was heated above~35°C. For GumC-His, cross-linking experiments were carried out to investigate whether the first section of the melting curve corresponded to protein aggregation. As the temperature increased, the protein bands gradually disappeared as high molecular mass aggregates formed that could not enter the gel and that were easy to see at temperatures above ~45°C [Fig. 4(F)].

To investigate whether xanthan induces conformational changes in these proteins, we analyzed GumB-His and GumC-His by far-UV CD spectroscopy in the presence of this polysaccharide. The shapes of the GumB-His spectra with versus without 0.01% xanthan were similar. However, in the presence of xanthan, the GumB-His signal was 15% more intense [Fig. 4(A)]. To investigate whether xanthan stabilizes GumB-His, we subjected GumB-His to thermal denaturation in the presence of 0.01% xanthan. GumB-His thermal unfolding was irreversible, and the melting points were similar regardless of the presence of xanthan [Fig. 4(C)], suggesting that the thermal stability of GumB-His was not modified by xanthan. We observed no changes in the far-UV CD spectrum of GumC-His in the presence of xanthan; similarly, the melting curve did not change [Fig. 4(B) and (D)].

Figure 4

Susceptibility of GumB-His and GumC-His to proteolysis

To investigate the degree of exposure of the flexible regions of GumB-His and GumC-His, we digested both purified proteins with trypsin. GumB-His was highly resistant to digestion by trypsin, leading to a predominant ~17-kDa fragment [Fig. 5(A)]. After 24 h of digestion, only ~20–30% of the GumB-His had been digested by trypsin. In contrast, GumC-His was very susceptible to proteolysis by trypsin, with a 5-min digestion producing two predominant fragments that corresponded to bands of ~45 kDa and ~23 kDa [Fig. 5(B)].

The structure and dynamics of the substrate protein play crucial roles in limiting proteolysis, and different conformations of the same protein can show different susceptibilities to proteolysis [31,32]. Because conformational changes can result in the exposure of previously protected protein regions to protease cleavage, we investigated whether GumB-His and/or GumC-His underwent such conformational changes in presence of xanthan. We found that the proteolytic pattern of GumB-His and GumC-His were similar in the absence and in presence of 0.01% xanthan [Fig. 5(C) and (D)].

Figure 5

Role of the TMSs of GumC in its expression and/or stabilization and oligomerization

To investigate whether the TMSs of GumC contribute to protein expression and/or stabilization and oligomerization, we analyzed two truncated proteins: $GumC_{53\text{-}472}$, which lacks the N-terminal TMS, and $GumC_{1\text{-}447}$, which lacks the C-terminal TMS. Each truncated protein lacks only one TMS; therefore, we could analyze the individual effect of each TMS. The $gumC_{53\text{-}472}$ and $gumC_{1\text{-}447}$ genes, which were cloned into the pBBRprom vector (Table I), were expressed in the Xc3188C/pXanA *gumC* mutant [Fig. 6(A)]. Despite the loss of the N-terminal TMS, immunoblot analysis showed that $GumC_{53\text{-}472}$ was still expressed, although its expression level was lower than that observed for GumC. In contrast, $GumC_{1\text{-}447}$ was not expressed or was expressed at undetectable levels or was immediately degraded, suggesting

that the C-terminal TMS is critical for GumC expression. *In vivo* cross-linking with DSP showed that the absence of the N-terminal TMS interfered with the ability of GumC to form oligomers [Fig. 6(B)]. $GumC_{53-472}$ did not form any type of oligomers or complexes in the presence of DSP, at least not at levels that were detectable by immunoblotting.

Figure 6

DISCUSSION

GumB and GumC are the outer membrane polysaccharide export (OPX) and the polysaccharide co-polymerase (PCP) proteins, respectively, of the xanthan biosynthesis system. They were classified as members of these families by *in silico* analysis [1], and there are no experimental data that confirm these roles. To study GumB and GumC, we overexpressed them as recombinant proteins and we were able to overexpress and purify GumB-His that lacked its signal peptide and full-length GumC-His [Fig. 1].

In this study, the results of the *in vitro* chemical cross-linking, SEC-SLS [Fig. 2], and AUC SV [Fig. 3] experiments indicated that purified GumB-His could form oligomers up to tetramer in solution. Jacobs et al. [21] reported that GumB-His crystals that were analyzed by X-ray diffraction also showed an oligomeric state corresponding to a tetrameric protein. The GumB-His quaternary structure was determined unequivocally in solution and the results were consistent. We could not determine the *in vivo* oligomeric state of native GumB (data not shown). We think it is possible that, in its native environment, GumB forms a high molecular mass complex that transports nascent xanthan chains across the periplasm and/or the outer membrane. This large "transporter" could be formed by homo- oligomers of GumB and/or by the interaction of GumB with other XcFC2 protein(s). It has been reported that Wza forms octameric species [19] and that it interacts with Wzc to form a protein complex that can translocate the capsular polysaccharide to the bacterial surface [33,34]. McNulty et al. [35]

demonstrated that KpsD (OPX) and KpsE (PCP) form a multi- protein complex with other proteins; one of them, RhsA, seems to couple the biosynthesis and export of capsular polysaccharide group 2. Some evidence indicates that GumB may interact with GumC. For example, XcFC2 cells that co-express multiple copies of GumB and GumC also synthesize 2.5-fold longer xanthan chains than wild-type XcFC2 cells [16]. Although this may indicate an interaction between GumB and GumC, further studies are required to determine whether GumB and GumC form homo- and/or hetero-oligomers *in vivo*.

Although the *in vitro* chemical cross-linking results indicated that GumC-His forms oligomers, the SEC-SLS results were not determinant and did not allow us to confirm the oligomeric state of this protein in solution [Fig. 2]. Further analysis by AUC SV experiments indicated that GumC-His was mainly a monomeric protein in solution; however, ~15% of the signal corresponded to dimers [Fig. 3]. Keeping in mind that other purified PCP proteins studied to date form oligomers [36-42], we considered two possible explanations for our results. One is that in solution, GumC-His is principally a monomeric protein with *in vitro* structure that differs from that of other PCP proteins. The other possible explanation is that GumC does not form stable oligomers outside its native environment. In order to investigate whether extracting GumC-His from the inner membrane affects its stability, we performed *in vivo* cross-linking experiments [Fig. 2]. Immunoblot analysis of cross-linked extracts of the wild-type XcFC2 strain and in the mutant Xc3188C strain complemented with pBBad-CHis probed with anti-GumC showed that both GumC and GumC-His oligomerize. However, these results did not reveal whether GumC forms homo- or hetero-oligomers. As discussed for GumB, it is possible that GumC is part of a large complex composed of different proteins that allows xanthan transport across the bacterial wall. Note that if we consider the possibility that GumC forms *in vivo* hetero-oligomers with GumB, these complexes should be detected on immunoblots probed with the anti-GumB antibody. No such immunoreactive bands were

detected. We speculate that if GumB and GumC do interact, the complexes they form are too large to enter the SDS-PAGE gels; however, GumC could be forming homo-oligomers and/or complexes with Xc protein(s) other than GumB. Using *in vivo* cross-linking with formaldehyde, Guo et al. [40] showed that Wzz_{86} forms very large complexes (>250-kDa). However, that report did not state whether the complexes were homo- or hetero-oligomers.

The TMSs are important for GumC stabilization and/or folding. In general, TMS are important for the correct localization of membrane proteins. However, it is possible that the TMS have another function as well. For example, there is evidence that they play a role in the oligomerization of other PCP proteins [38,39]. For this reason, we studied two truncated proteins: $GumC_{53-472}$ and $GumC_{1-447}$ [Fig. 6]. Neither Xc3188C/pBBR-promC_{53-472} nor Xc3188C/pBBRprom-C_{1-447} strains produced xanthan (data not shown). The absence of the N-terminal TMS affected GumC expression and oligomerization. We did not observe a band corresponding to $GumC_{1-447}$ on the immunoblots. Thus, either the absence of the C-terminal TMS greatly decreased or abolished protein expression or, alternatively, $GumC_{1-447}$ was immediately degraded after translation. In any case, the TMSs seemed to play an important role in GumC stability.

These findings suggest that the N-terminal TMS is involved in GumC expression and oligomerization, and the inability of Xc3188C/pBBRprom-C_{53-472} cells to produce xanthan indicates that GumC oligomerization is required for its function. The C-terminal TMS seems to be important for GumC synthesis and/or stability. In contrast with our results, Daniels & Morona [38] reported that C-terminal-truncated Wzz_{SF} forms oligomers, suggesting that the N-terminal region of this protein is sufficient for Wzz_{SF}-Wzz_{SF} interaction. This report also noted that the N-terminal TMS is implicated in Wzz_{SF} dimerization. On the other hand, site-directed mutagenesis studies of residues in the C-terminal TMS of ExoP have shown that

these mutations affect succinoglycan synthesis, suggesting that this TMS is important for ExoP function [43]. Laure et al. [39] reported that three full-length Wzz proteins form hexamers, while Tocilj et al. [37] observed that the periplasmic regions of these proteins form pentamers, octamers, and hexamers, showing the importance of the TMSs of PCP proteins for their oligomerization and/or function.

The far-UV CD spectrum shape revealed that GumC-His has a predominantly α- helical secondary structure and that GumB-His is not only composed of β-sheet [Fig.4] as described for other outer membrane auxiliary proteins [44]. Our results are consistent with *in silico* predictions. GumB-His thermal denaturation seemed to follow a simple, cooperative, and irreversible two-state denaturation process [Fig. 4]. Because GumB-His is an oligomeric protein, we expected to observe an additional transition in its thermal unfolding, corresponding to the loss of its quaternary structure, but the native tetrameric GumB-His was quickly converted into an unfolded protein with a relatively low apparent melting temperature. GumB-His thermal unfolding was irreversible due to protein aggregation [Fig. 4]. Based on this result, we think that GumB-His is a compact protein that immediately unfolds when it loses its quaternary structure. This rapid denaturation, which exposes hydrophobic regions, could be responsible for irreversible aggregation of GumB-His. Limited proteolysis experiments support the hypothesis that GumB-His is a compact protein. After incubation of GumB-His with trypsin, we observed its high resistance to digestion [Fig. 5].

In contrast, we observed a non-cooperative and irreversible thermal unfolding process for GumC-His [Fig. 4]. The transition between the native and the unfolded states indicated the formation of partially unfolded intermediate(s). This type of melting curves is generally observed for oligomeric proteins; loss of quaternary structure is reflected in the melting curve as an intermediate stage between the native and the completely unfolded states. The AUC

results indicated that GumC-His is predominantly a monomeric protein; therefore, we think the unfolding transition between 10 to 60°C corresponds to a GumC-His state that retains significant secondary structure but lacks stable tertiary structure. The far-UV CD spectrum showed that GumC-His has a stable secondary structure; but the weak near-UV CD spectrum suggests that GumC-His has a flexible and/or elongated tertiary structure (data not shown). If we assume that GumC-His has extended or flexible regions, we can attribute the first denaturation transition to the unfolding of these flexible regions and the second transition (above 50°C) to the loss of the remaining secondary structure. The thermal denaturation of GumC-His is also an irreversible process due to protein aggregation and by the formation of protein complexes that did not enter the SDS-PAGE gel after cross-linking with DSP at temperatures above 50°C [Fig. 4]. As discussed for GumB-His, this irreversible aggregation could be due to the exposure of hydrophobic regions when the temperature is increased. The proteolysis profile of GumC-His [Fig. 5] also support our hypothesis that GumC-His has extended solvent-exposed regions that can be cleaved by proteases, can bind solvent components (i.e. DDM micelles), and that allow GumC-His to interact with other monomers and/or other protein(s). As we observed for the *in vivo* cross-linking experiments, GumC forms oligomers in its native environment [Fig. 2], and these extended regions may be involved in GumC oligomerization.

Because GumB and GumC are involved in the polymerization and export of xanthan, we investigated whether these proteins undergo conformational changes in the presence of this polysaccharide. Accordingly, we analyzed the far-UV CD spectra of GumB-His and GumC-His alone and with xanthan [Fig. 4]. We did not observe changes in the shapes of the far-UV CD spectra of either GumB-His or GumC-His; however, the intensity of the signal of GumB-His spectrum increased in the presence of xanthan. Based on this result, we wondered whether GumB-His interacted with xanthan and whether such an interaction modified its stability. To

investigate this, we carried out thermal denaturation of GumB-His incubated with xanthan, expecting to see changes in the melting curve [Fig. 4]. However, the melting point was unchanged. In addition, we subjected GumB-His and GumC-His, either alone or with xanthan, to limited proteolysis with trypsin. The digestion profiles did not change [Fig. 5]. These results suggest that if GumB-His and xanthan interact, the interaction does not affect protein stability. In the case of Gumc-His, xanthan does not modify its secondary structure nor does it expose or block the flexible regions. This suggests that there is no interaction between the protein and the polysaccharide in these experimental conditions.

The behavior of GumC in the presence of xanthan contrasts with that reported for Wzz_{86} in the presence of O-antigen. The far-UV CD spectrum of Wzz_{86} shows a significantly change in presence of O-antigen [40], and SAXS experiments also show that Wzz_{86} has an apparent O-antigen-induced conformational change [41].

The results presented here lay the groundwork for future studies that will clarify the roles of GumB and GumC in xanthan polymerization and export.

ACKNOWLEDGMENTS

We are grateful to María S. Malori for technical assistance with high-pressure liquid chromatography and to Marta Bravo for technical assistance with DNA sequencing. This study used the platforms at the Grenoble Instruct Centre (ISBG; UMS 3518 CNRS-CEA-UJF-EMBL) with support from FRISBI (ANR-10-INSB-05-02) and GRAL (ANR-10-LABX-49-01) within the Grenoble Partnership for Structural Biology (PSB). We thank Dr. Christine Ebel of the AUC platform. This study was supported by the Agencia Nacional de Promoción Científica y Tecnológica (ANPCyT) [PICT 1/2452] (Argentina) and the Consejo Nacional de Investigaciones Científicas y Técnicas (CONICET) [PIP 399] (Argentina). MIB and LI are Career Investigators supported by CONICET (Argentina), and MJ and SRS are supported by CONICET doctoral fellowships.

FIGURE LEGENDS

Figure 1. Overexpression and purification of GumB-His and GumC-His. (A) Immunoblots of the GumB-His purification using anti-GumB antibody. (B) Coomassie blue-stained SDS-PAGE analysis of the overexpression and purification of GumC-His by nickel affinity (Ni+) and size-exclusion (SEC) chromatography. Immunoblot of the GumC-His purification using anti-GumC antibody. The black and grey arrowheads point to GumB-His and GumC-His, respectively.

Figure 2. The oligomeric state of GumB-His and GumC-His. Coomassie Blue stained SDS-PAGE gel of *in vitro* cross-linked GumB-His (A) and GumC-His (B). (C) Active wild-type XcFC2 cells were subjected to *in vivo* chemical cross-linking with DSP and analyzed by immunoblot using an anti-GumC antibody. SEC-SLS profile of GumB-His (D) and GumC-His (E). The experiments were performed with a flow rate of 0.4 ml/min. (F and G) Molecular mass determination of purified GumC-His. m/z values obtained by MALDI-TOF MS match closely to the predicted molecular mass. In panels A, B, and C, the black and white arrowheads indicate monomers and oligomers, respectively.

Figure 3. The oligomeric state of GumB-His and GumC-His as determined by AUC SV analysis. (A) The main contribution of GumB-His was detected at ~4.9 S and the secondary contribution at ~7.1 S. (B) The main contribution of GumC-His was detected at ~2 S with a shoulder at ~3 S. For both proteins, the *c(s)* distributions were normalized to the maximum value of the pick above 1.5 S. The signal was normalized to a 1-cm optical path length.

Figure 4. Secondary structure and thermal unfolding of GumB-His and GumC-His. GumB-His (A) and GumC-His (B) far-UV CD spectra. GumB-His (C) and GumC-His (D) were subjected to thermal denaturation followed by far-UV CD analysis (dashed black line) and turbidity analysis (black line), recorded at 216 nm and 222 nm, respectively. Thermal

denaturation of GumB-His (C) and GumC-His (D) incubated with xanthan (grey line). All CD spectra were collected at 20ºC, and similar results were obtained at 5ºC. The CD measurements of each protein were repeated at least three times. The GumB-His and GumC-His spectra were baseline-corrected with buffer or buffer containing 0.01% xanthan. The stability of GumB-His (E) and GumC-His (F) as a function of temperature was analyzed by chemical cross-linking with DSP (panel a) and with the addition of DTT as a control (panel b).

Figure 5. Limited proteolysis of GumB-His and GumC-His. Profiles of GumB-His (A) and GumC-His (B) after digestion with trypsin. Profiles of GumB-His (C) and GumC-His (D) after digestion with trypsin in presence of 0.01% xanthan. The black arrowheads indicate undigested GumB- His and GumC-His, while white arrowheads point to the digestion products.

Figure 6. The expression, subcellular localization, and oligomeric state of GumC mutant proteins lacking transmembrane segments. (A) Immunoblot analysis of *in vivo* cross- linking using an anti-GumC antibody. Total cell extracts of Xc3188C/pXanA/pBBRprom (lane 1), Xc3188/pXanA/pBBRprom (lane 2), Xc3188C/pXanA/pBBRpromC (lane 3), Xc3188C/pXanA/pBBRpromC$_{53\text{-}472}$ (lane 4), and Xc3188C/pXanA/pBBRpromC$_{1\text{-}447}$ (lane 5). (B) Immunoblot analysis of the membrane fraction of Xc3188C/pXanA/pBBRpromC cells (lane 6), Xc3188C/pXanA/pBBRpromC$_{53\text{-}472}$ cells (lane 7), and Xc3188C/pXanA/pBBRpromC$_{1\text{-}447}$ cells (lane 8); and of the total cell extract from Xc3188C/pXanA/pBBRpromC$_{53\text{-}472}$ cells (lane 9) and Xc3188C/pXanA/pBBRpromC$_{1\text{-}447}$ cells (lane 10). Black arrowheads indicate GumC and C$_{53\text{-}472}$ monomers, while white arrowheads indicate GumC oligomers.

REFERENCES

[1] Cuthbertson L, Mainprize IL, Naismith JH, Whitfield C (2009) Pivotal roles of the outer membrane polysaccharide export and polysaccharide copolymerase protein families in export of extracellular polysaccharides in gram-negative bacteria. Microbiol Mol Biol Rev 73:155-177.

[2] Yun MH, Torres PS, El Oirdi M, Rigano LA, Gonzalez-Lamothe R, Marano MR, Castagnaro AP, Dankert MA, Bouarab K, Vojnov AA (2006) Xanthan induces plant susceptibility by suppressing callose deposition. Plant Physiol 141:178-187.

[3] Dow JM, Crossman L, Findlay K, He YQ, Feng JX, Tang JL (2003) Biofilm dispersal in *Xanthomonas campestris* is controlled by cell-cell signaling and is required for full virulence to plants. Proc Natl Acad Sci U S A 100:10995-11000.

[4] Dow JM, Crossman L, Findlay K, He YQ, Feng JX, Tang JL (2003) Biofilm dispersal in *Xanthomonas campestris* is controlled by cell-cell signaling and is required for full virulence to plants. Proc Natl Acad Sci U S A 100:10995-11000.

[5] Jansson PE, Kenne L, Lindberg B (1975) Structure of extracellular polysaccharide from *Xanthomonas campestris*. Carbohydr Res 45:275-282.

[6] Becker A, Katzen F, Puhler A, Ielpi L (1998) Xanthan gum biosynthesis and application: a biochemical/genetic perspective. Appl Microbiol Biotechnol 50:145-152.

[7] Kanegasaki S & Wright A (1970) Mechanism of polymerization of the Salmonella O-antigen: utilization of lipid-linked intermediates. Proc Natl Acad Sci U S A 67:951-958.

[8] Woodward R, Yi W, Li L, Zhao G, Eguchi H, Sridhar PR, Guo H, Song JK, Motari E, Cai L, Kelleher P, Liu X, Han W, Zhang W, Ding Y, Li M, Wang PG (2010) In vitro bacterial polysaccharide biosynthesis: defining the functions of Wzy and Wzz. Nat Chem Biol 6:418-423.

[9] Katzen F, Becker A, Zorreguieta A, Puhler A, Ielpi L (1996) Promoter analysis of the *Xanthomonas campestris* pv. *campestris* gum operon directing biosynthesis of the xanthan polysaccharide. J Bacteriol 178:4313-4318.

[10] Capage MA, Doherty DH, Betlach MR, Vanderslice RW (1987) Recombinant-DNA mediated production of xanthan gum. International patent WO 87/05938.

[11] Barreras M, Abdian PL, Ielpi L (2004) Functional characterization of GumK, a membrane-associated beta-glucuronosyltransferase from *Xanthomonas campestris* required for xanthan polysaccharide synthesis. Glycobiology 14:233-241.

[12] Barreras M, Salinas SR, Abdian PL, Kampel MA, Ielpi L (2008) Structure and mechanism of GumK, a membrane-associated glucuronosyltransferase. J Biol Chem 283:25027-25035.

[13] Ielpi L, Couso RO, Dankert MA (1993) Sequential assembly and polymerization of the polyprenol-linked pentasaccharide repeating unit of the xanthan polysaccharide in *Xanthomonas campestris*. J Bacteriol 175:2490-2500.

[14] Katzen F, Ferreiro DU, Oddo CG, Ielmini MV, Becker A, Pühler A, Ielpi L (1998) *Xanthomonas campestris* pv. *campestris* gum Mutants: Effects on Xanthan Biosynthesis and Plant Virulence. J Bacteriol 180:1607-1617.

[15] Salinas SR, Bianco MI, Barreras M, Ielpi L (2011) Expression, purification and biochemical characterization of GumI, a monotopic membrane GDP-mannose:glycolipid 4-{beta}-D-mannosyltransferase from *Xanthomonas campestris* pv. *campestris*. Glycobiology 21:903-913.

[16] Galvan EM, Ielmini MV, Patel YN, Bianco MI, Franceschini EA, Schneider JC, Ielpi L (2013) Xanthan chain length is modulated by increasing the availability of the polysaccharide copolymerase protein GumC and the outer membrane polysaccharide export protein GumB. Glycobiology 23:259-272.

[17] Vojnov AA, Zorreguieta A, Dow JM, Daniels MJ, Dankert MA (1998) Evidence for a role for the gumB and gumC gene products in the formation of xanthan from its pentasaccharide repeating unit by *Xanthomonas campestris.* Microbiology 144:1487-1493.

[18] Sathiyamoorthy K, Mills E, Franzmann TM, Rosenshine I, Saper MA (2011) The crystal structure of *Escherichia coli* group 4 capsule protein GfcC reveals a domain organization resembling that of Wza. Biochemistry 50:5465-5476.

[19] Dong C, Beis K, Nesper J, Brunkan-Lamontagne AL, Clarke BR, Whitfield C, Naismith JH (2006) Wza the translocon for *E. coli* capsular polysaccharides defines a new class of membrane protein. Nature 444:226-229.

[20] Morona R, Van Den Bosch L, Daniels C (2000) Evaluation of Wzz/MPA1/MPA2 proteins based on the presence of coiled-coil regions. Microbiology 146:1-4.

[21] Jacobs M, Salinas SR, Bianco MI, Ielpi L (2012) Expression, purification and crystallization of the outer membrane lipoprotein GumB from *Xanthomonas campestris.* Acta Crystallogr Sect F Struct Biol Cryst Commun 68:1255-1258.

[22] Sambrook J, Fritsch EF, Maniatis T (1989) Molecular Cloning: a Laboratory Manual (Cold Spring Harbor Laboratory Press, Cold Spring Harbor, N. Y.) 2nd Ed.

[23] Harding NE, Raffo S, Raimondi A, Cleary JM, Ielpi L (1993) Identification, genetic and biochemical analysis of genes involved in synthesis of sugar precursors in xanthan gum. J Gen Microbiol 139:447-457.

[24] Patel Y, Schneider JC, Ielpi L, Ielmini MV (2008) High viscosity Xanthan Polymer Preparations in US: 7,439,044 B2.

[25] Slotboom DJ, Duurkens RH, Olieman K, Erkens GB (2008) Static light scattering to characterize membrane proteins in detergent solution. Methods 46:73-82.

[26] Prossnitz E, Nikaido K, Ulbrich SJ, Ames GF (1988) Formaldehyde and photoactivatable cross-linking of the periplasmic binding protein to a membrane component of the histidine transport system of *Salmonella typhimurium*. J Biol Chem 263:17917-17920.

[27] Zgurskaya HI & Nikaido H (2000) Cross-linked complex between oligomeric periplasmic lipoprotein AcrA and the inner-membrane-associated multidrug efflux pump AcrB from *Escherichia coli*. J Bacteriol 182:4264-4267.

[28] Salvay AG, Le Maire M, Ebel C. (2007) Analytical ultracentrifugation sedimentation velocity for the characterization of detergent-solubilized membrane proteins Ca^{++}-ATPase and ExbB. J Biol Phys 33:399-419.

[29] Santoro MM & Bolen DW (1988) Unfolding free energy changes determined by the linear extrapolation method. 1. Unfolding of phenylmethanesulfonyl alpha-chymotrypsin using different denaturants. Biochemistry 27:8063-8068.

[30] Salvay AG & Ebel C (2006) Analytical ultracentrifuge for the characterization of detergents in solutions. Prog Colloid Polym Sci 131:74-82.

[31] Tsai CJ, Polverino de Laureto P, Fontana A, Nussinov R (2002) Comparison of protein fragments identified by limited proteolysis and by computational cutting of proteins. Prot Sci 11: 1753-1770.

[32] Fontana A, de Laureto PP, Spolaore B, Frare E, Picotti P, et al. (2004) Probing protein structure by limited proteolysis. Acta Biochim Pol 51: 299-321.

[33] Collins RF, Beis K, Dong C, Botting CH, McDonnell C, Ford RC, Clarke BR, Whitfield C, Naismith JH (2007) The 3D structure of a periplasm-spanning platform required for assembly of group 1 capsular polysaccharides in *Escherichia coli*. Proc Natl Acad Sci U S A 104:2390-2395.

[34] Nesper J, Hill CM, Paiment A, Harauz G, Beis K, Naismith JH, Whitfield C (2003) Translocation of group 1 capsular polysaccharide in *Escherichia coli* serotype K30. Structural and functional analysis of the outer membrane lipoprotein Wza. J Biol Chem 278:49763-49772.

[35] McNulty CT, Thompson J, Barrett B, Lord L, Andersen C, Roberts IS (2006) The cell surface expression of group 2 capsular polysaccharides in *Escherichia coli*: the role of KpsD, RhsA and a multi-protein complex at the pole of the cell. Mol Microbiol 59:907-922.

[36] Collins RF, Beis K, Clarke BR, Ford RC, Hulley M, Naismith JH, Whitfield C (2006) Periplasmic protein-protein contacts in the inner membrane protein Wzc form a tetrameric complex required for the assembly of *Escherichia coli* group 1 capsules. J Biol Chem 281:2144-2150.

[37] Tocilj A, Munger C, Proteau A, Morona R, Purins L, Ajamian E, Wagner J, Papadopoulos M, Van Den Bosch L, Rubinstein JL, Fethiere J, Matte A, Cygler M (2008) Bacterial polysaccharide co-polymerases share a common framework for control of polymer length. Nat Struc Mol Biol 15:130-138.

[38] Daniels C & Morona R (1999) Analysis of *Shigella flexneri* wzz (Rol) function by mutagenesis and cross-linking: wzz is able to oligomerize. Mol Microbiol 34:181-194.

[39] Larue K, Kimber MS, Ford R, Whitfield C (2009) Biochemical and structural analysis of bacterial O-antigen chain length regulator proteins reveals a conserved quaternary structure. J Biol Chem 284:7395-7403.

[40] Guo H, Lokko K, Zhang Y, Yi W, Wu Z, Wang PG (2006) Overexpression and characterization of Wzz of *Escherichia coli* O86:H2. Protein Expr Purif 48:49-55.

[41] Tang KH, Guo H, Yi W, Tsai MD, Wang PG (2007) Investigation of the conformational states of Wzz and the Wzz.O-antigen complex under near-physiological conditions. Biochemistry 46:11744-11752.

[42] Papadopoulos M & Morona R (2010) Mutagenesis and chemical cross-linking suggest that Wzz dimer stability and oligomerization affect lipopolysaccharide O-antigen modal chain length control. J Bacteriol 192:3385-3393.

[43] Becker A & Puhler A (1998) Specific amino acid substitutions in the proline-rich motif of the *Rhizobium meliloti* ExoP protein result in enhanced production of low-molecular-weight succinoglycan at the expense of high-molecular-weight succinoglycan. J Bacteriol 180:395-399.

[44] Paulsen IT, Beness AM, Saier MH Jr. (1997) Computer-based analyses of the protein constituents of transport systems catalysing export of complex carbohydrates in bacteria. Microbiology 143:2685-2699.

[45] Ielmini MV (2007) Genética molecular y bioquímica de la síntesis de exopolisacáridos bacterianos. Doctoral Thesis (University of Buenos Aires, Buenos Aires, Argentina).

[46] Sukchawalit R, Vattanaviboon P, Sallabhan R, and Mongkolsuk S (1999) Construction and characterization of regulated L-arabinose-inducible broad host range expression vectors in *Xanthomonas*. FEMS Microbiol Lett 181:217-223.

[47] Vilas G & Ielpi L (2000) Unpublished results.

[48] Kidby D, Sandford P, Herman A, Cadmus M (1977) Maintenance procedures for the curtailment of genetic instability: *Xanthomonas campestris* NRRL B-1459. Appl Environ Microbiol 33:840-845

[49] Köplin R, Arnold W, Hötte B, Simon R, Wang G, Pühler A (1992) Genetics of xanthan production in *Xanthomonas campestris*: the *xanA* and *xanB* genes are involved in UDP-glucose and GDP-mannose biosynthesis. J Bacteriol. 174:191–199.

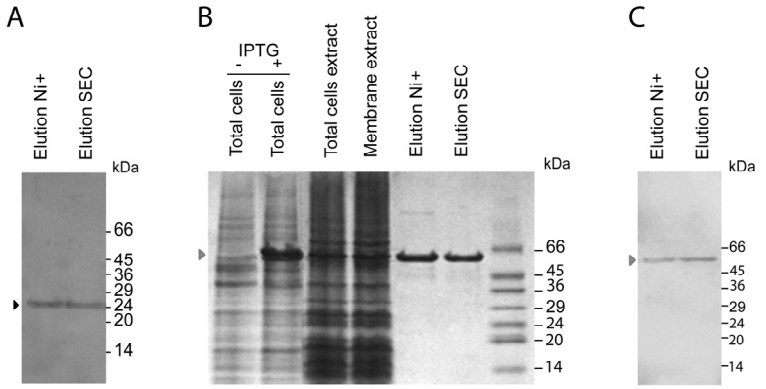

Fig. 1

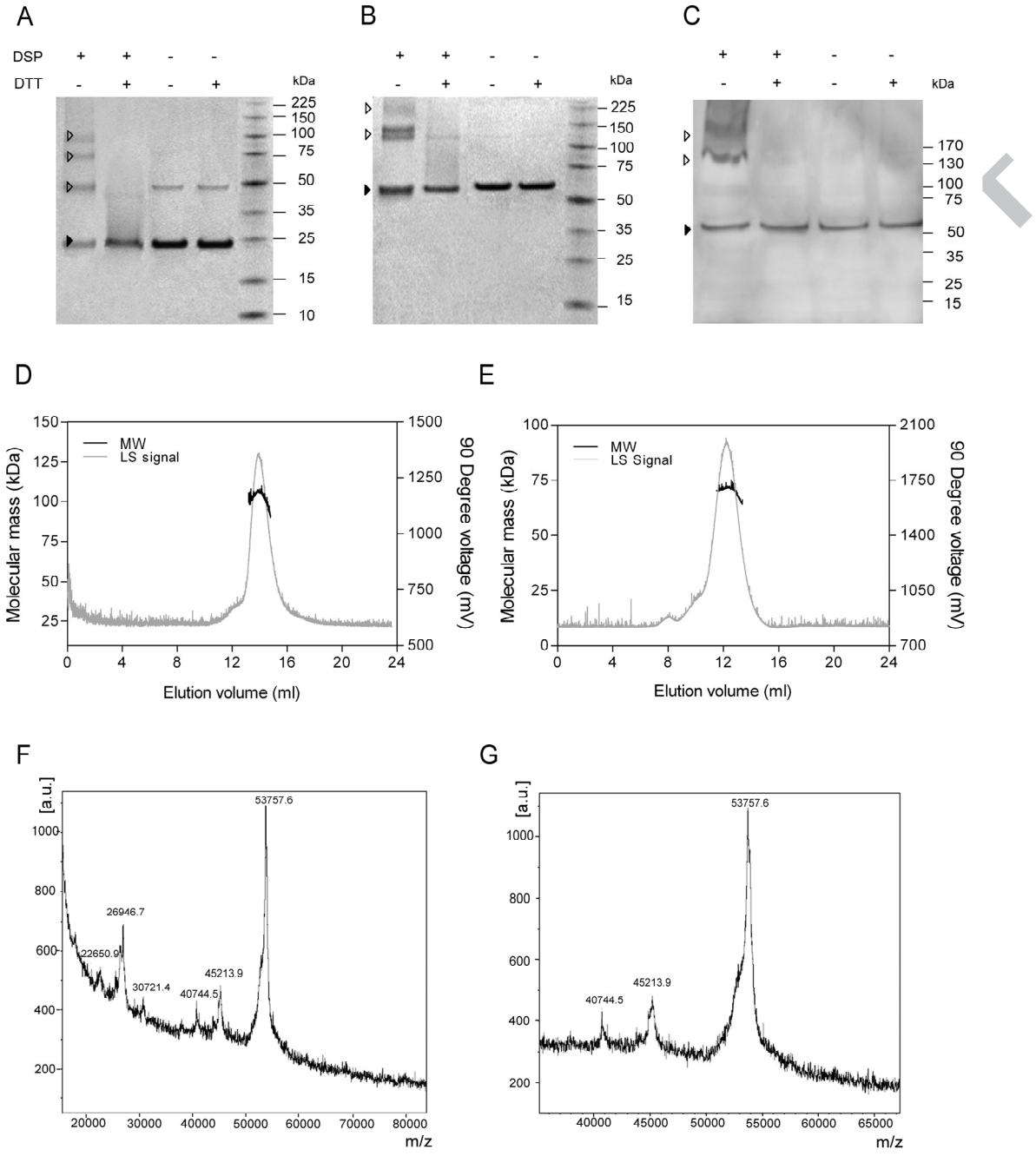
A
DSP + + - -
DTT - + - +
kDa
225
150
100
75
50
35
25
15
10
B
+ + - -
- + - +
kDa
225
150
100
75
50
35
25
15
C
+ + - -
- + - +
kDa
170
130
100
75
50
35
25
15
D
MW
LS signal
Molecular mass (kDa)
90 Degree voltage (mV)
Elution volume (ml)
E
MW
LS Signal
Molecular mass (kDa)
90 Degree voltage (mV)
Elution volume (ml)
F
[a.u.]
53757.6
26946.7
22650.9
30721.4
40744.5
45213.9
m/z
G
[a.u.]
53757.6
40744.5
45213.9
m/z

Fig. 2

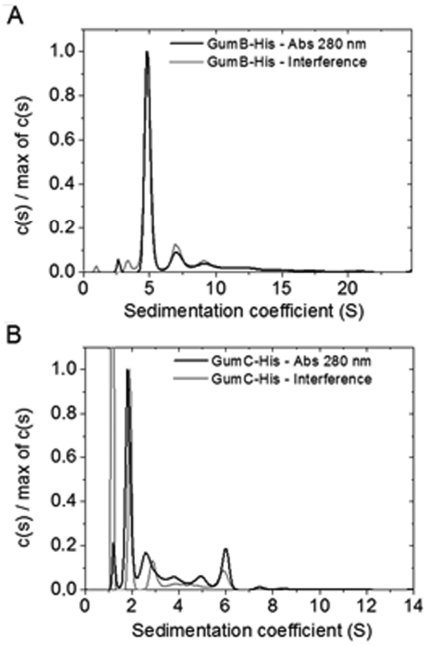

Fig. 3

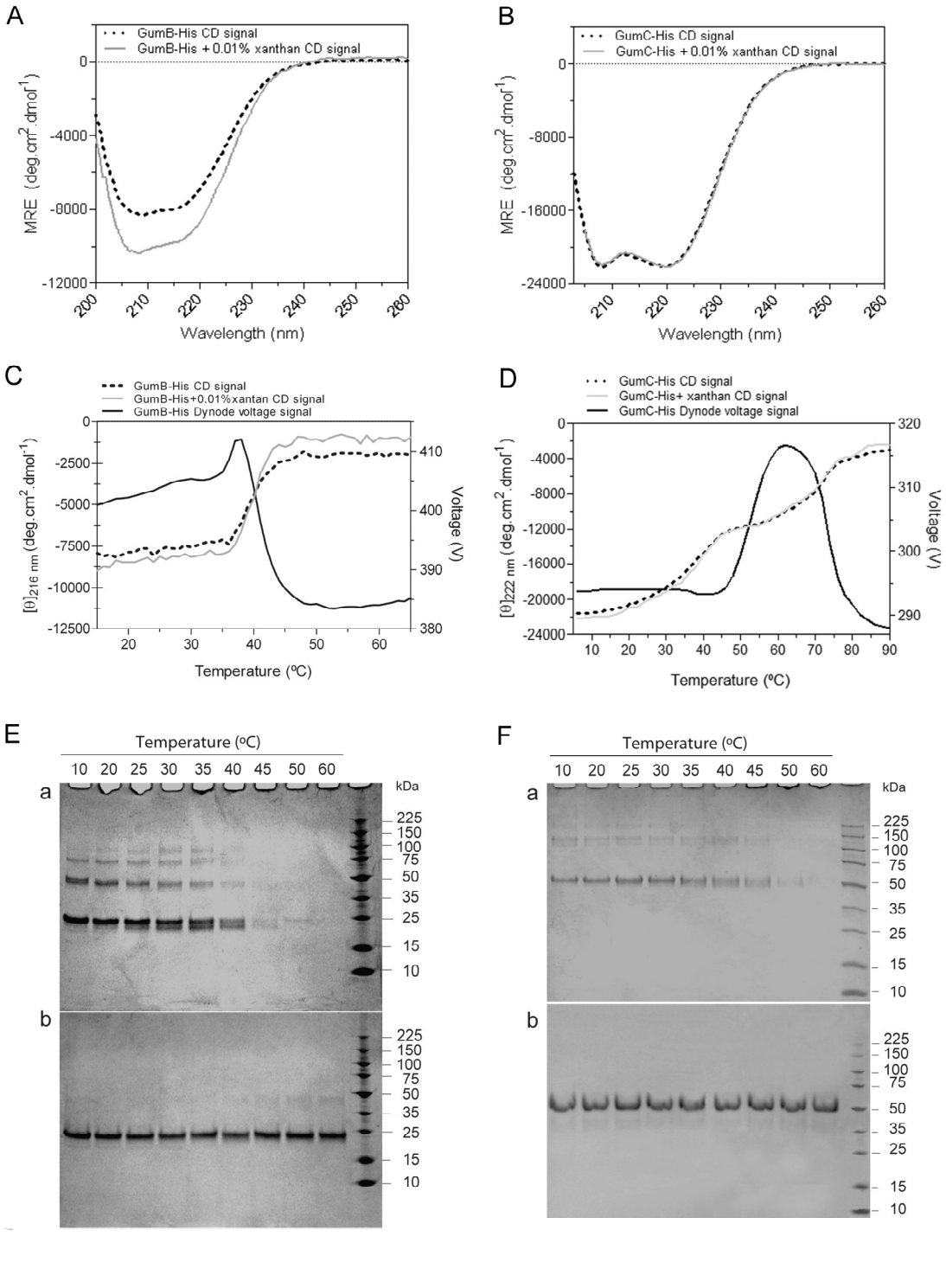
A
GumB-His CD signal
GumB-His + 0.01% xanthan CD signal
MRE (deg.cm2.dmol-1)
Wavelength (nm)
B
GumC-His CD signal
GumC-His + 0.01% xanthan CD signal
MRE (deg.cm2.dmol-1)
Wavelength (nm)
C
GumB-His CD signal
GumB-His+0.01%xantan CD signal
GumB-His Dynode voltage signal
[θ]216 nm (deg.cm2.dmol-1)
Voltage (V)
Temperature (ºC)
D
GumC-His CD signal
GumC-His+ xanthan CD signal
GumC-His Dynode voltage signal
[θ]222 nm (deg.cm2.dmol-1)
Voltage (V)
Temperature (ºC)
E
Temperature (ºC)
10 20 25 30 35 40 45 50 60
a
b
kDa
225
150
100
75
50
35
25
15
10
F
Temperature (ºC)
10 20 25 30 35 40 45 50 60
a
b
kDa
225
150
100
75
50
35
25
15
10

Fig. 4

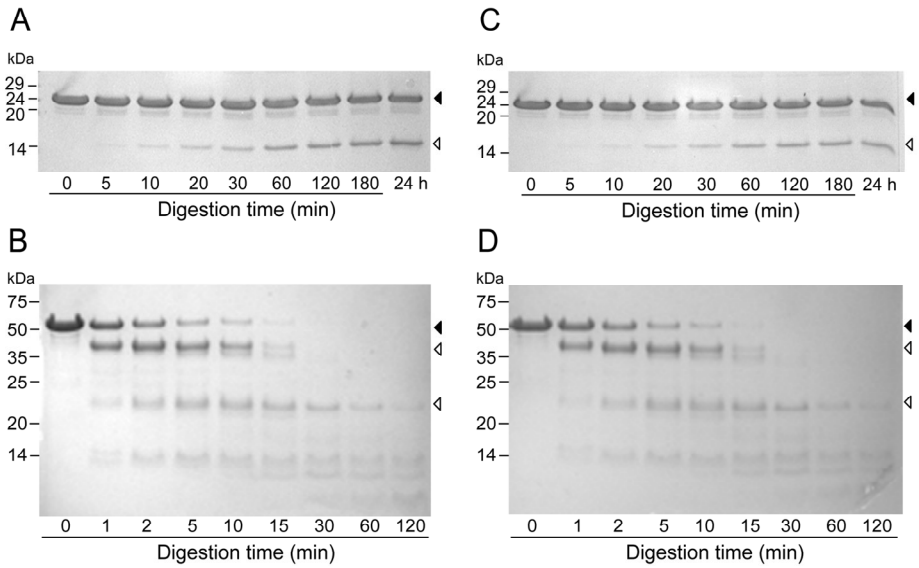

Fig. 5

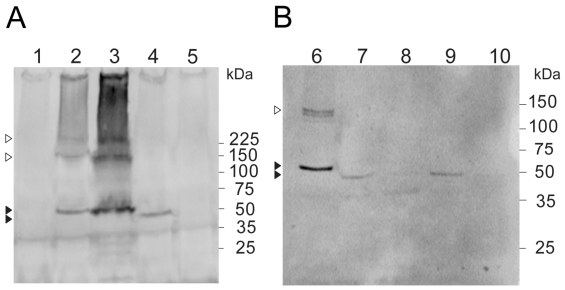

Fig. 6

Table I. *X. campestris* strains and plasmids used in this study.

	Characteristics	Reference
Strains		
XcFC2	Rif^r derived from wild-type NRRL B-1459[a]	[14]
Xc3188[b]	NRRL B-1459 derivative 0100 *pgm* Rif^r	[23]
Xc3188C	Xc3188 Δ*gumC*	[45]
Plasmids		
pET28a(+)	Km^r	Promega
pBBad22K	Overexpression broad-host range vector containing the BAD promoter, the pBBR1-MCS-4 replicon, and Km^r	[46]
pBBad22T	Overexpression broad-host range vector containing the BAD promoter, the pBBR1-MCS-4 replicon, and Tc^r	[46]
pBBR5-BC	pBBR1-MCS-5 carrying the *gum* fragment 771-3611[c] upstream of the multiple cloning site	[45]
pQE30-GBHis	pQE30-XpsB#6: pQE30 vector carrying *gum* fragment 1336–1971[c] with a His_6-tag added at the N-terminal end	CP Kelco
pET-GCHis	pET28a(+) derivate carrying the *gumC* gene[d] and a His_6-tag at the C-terminal end	This study
pBBad-B	pBBad22T carrying the *gum*B gene[d]	[16]
pBBad-C	pBBad22K carrying the *gum*C gene[d]	[16]
pBBad-CHis	pBBad22K carrying the *gum*C gene[d] and a His_6-tag at the C-terminal end	This study
pREP4	Plasmid containing the repressor gene *lac*I and Km^r	Qiagen
pXanA	pRK404 derivate carrying the *xan*A gene[e] and Tc^r	[47]
pJC440	Plasmid based on pRK293 carrying the xpsIV region of *X. campestris*	[23]
pBBR-prom	pBBR1-MCS-5 carrying the *gum* promoter upstream of the multiple cloning site	[16]
pBBR-promC	pBBR-prom carrying the *gumC* gene[d]	[16]
pBBR-promC$_{53-472}$	pBBR-prom carrying the *gum* fragment 2135–3459[c]	[45]
	Fragment of the *gum*C gene digested with *NdeI*/*Kpn*I that lacks the first transmembrane segment that encodes the truncated protein $GumC_{53-472}$	
pBBR-promC$_{1-447}$	pBBR-prom carrying the *gum* fragment 1979–3319[c]	[45]
	Fragment of *gum*C gene digested with *NdeI*/*Kpn*I that lacks the second transmembrane segment that encodes the truncated protein $GumC_{1-447}$	

[a] NRRL B-1459: *Xc* wild type strain [48]
[b] Strain deficient in phosphomano-phosphoglucomutase activity. When required its absence was restored by the introduction of the pXanA plasmid
[c] Fragment of the *gum* region. Numbers correspond to positions in the nucleotide sequence of the *gum* region (GenBank accession number U22511).
[d] Numbers correspond to the position in the nucleotide sequence of the *gumB* gene (GenBank accession number AF427012) or the *gumC* gene (GenBank accession number AF427011).
[e] Responsible for phosphoglucomutase and phosphomanomutase activities [49]

Table II. Primers used in this study

Primer	Sequence
FGC28.HisCt	5'-CCATGGGGAATTCAGACAATCGTTCCTCTTCG-3' (*Nco*I site underlined)
RGC28.HisCt	5'-CCGCTCGAGGTTCAACCGCGACCTCGGAGAAG-3' (*Xho*I site underlined)
RGC22HisCt	5'-CCAAGCTTGGTCAGTGGTGGTGGTGGTG-3' (*Hind*III site underlined)

Highlights

- Characterization of GumB and GumC proteins involved in xanthan synthesis.
- The recombinant GumB shows to be a tetrameric protein.
- Native and recombinant GumC showed oligomeric conformation.
- GumC expression, stability and/or oligomerization rely on transmembrane segments.